A&A 487, 177–183 (2008)
DOI: 10.1051/0004-6361:200809660

Astronomy & Astrophysics

Stellar and dust properties of local elliptical galaxies: clues to the onset of nuclear activity *(Research Note)*

Y. Zhang[1], Q.-S. Gu[1], and L. C. Ho[2]

[1] Department of Astronomy, Nanjing University, Nanjing 210093, PR China
e-mail: zhangyu19842007@hotmail.com;qsgu@nju.edu.cn
[2] The Observatories of the Carnegie Institution of Washington, 813 Santa Barbara Street, Pasadena, CA 91101, USA
e-mail: lho@ociw.edu

Received 27 February 2008 / Accepted 4 June 2008

ABSTRACT

Aims. We study the stellar and dust properties of a well-defined sample of local elliptical galaxies to investigate the relationship between host galaxy properties and nuclear activity.
Methods. We have selected a complete sample of 45 ellipticals from the Palomar spectroscopic survey of nearby galaxies, which includes 20 low-luminosity active galactic nuclei classified as LINERs and 25 inactive galaxies. Using a stellar population synthesis method, we compared the derived stellar population properties of the LINER to the inactive subsamples. We also studied the dust and stellar surface brightness distributions of the central regions of these galaxies using high-resolution images obtained with the *Hubble Space Telescope*.
Results. Compared with the inactive subsample, ellipticals hosting LINERs share similar total optical and near-infrared luminosity, central stellar velocity dispersions, and nuclear stellar populations as judged from their luminosity-weighted ages and metallicities. LINERs, on the other hand, have a larger fraction of core-type central surface brightness profiles and a much higher frequency of circumnuclear dust structures.
Conclusions. Our results support the suggestion that LINERs are powered by low-luminosity AGNs rather than by young or intermediate-age stars. Nuclear activity in nearby elliptical galaxies seems to occur primarily in those systems where enough cold interstellar material has managed to accumulate, perhaps via cooling condensations from hot gas.

Key words. galaxies: elliptical and lenticular, cD – galaxies: active – galaxies: stellar content

1. Introduction

Supermassive black holes (SMBHs) are ubiquitous in elliptical galaxies. The discovery of a tight correlation between black hole mass and the stellar velocity dispersion of the bulge of the host galaxy (Gebhardt et al. 2000; Ferrarese & Merritt 2000) suggests that the formation and growth of central black holes are an integral part of the formation of galactic bulges. However, the majority of SMBHs in nearby ellipticals are not very active. In the Palomar spectroscopic survey of nearby galaxies (Ho et al. 1995, 1997a), only about 50% of the ellipticals show detectable emission-line nuclei, most of which (∼87%) are classified as low-ionization nuclear emission-line regions (LINERs; Heckman 1980; see Ho 2008, for a review).

The physical origin of LINERs has been intensively debated. A variety of recent observations, however, have provided convincing evidence that LINERs are low-luminosity active galactic nuclei (AGNs). This includes the detection of broad Hα emission (Ho et al. 1997b), some of which show double-peaked profiles (Ho et al. 2000; Shields et al. 2000; Barth et al. 2001) or are polarized (Barth et al. 1999a,b), ultraviolet variability (Maoz et al. 2005), compact X-ray cores (e.g., Ho et al. 2001; Terashima & Wilson 2003), and compact radio cores (e.g., Nagar et al. 2005). Ho (2008) suggests that nearly *all* LINERs are genuine AGNs with low accretion rates.

The low accretion rates of the SMBHs in nearby ellipticals probably stem from the lack of enough cold gas to fuel the central engine, as it is generally accepted that nearby elliptical galaxies contain mostly old stars and not much cold interstellar material. However, apart from the high detection rate of nuclear optical emission lines in spectroscopic surveys (Phillips et al. 1986; Ho et al. 1997a), Hα + [N II] narrow-band imaging has shown that elliptical galaxies certainly have plenty of extended warm (∼10^4 K) gas (e.g., Shields 1991). By coadding images from the *Infrared Astronomy Satellite* survey scans, Knapp et al. (1989) show that ∼50% of ellipticals contain cool dust. Temi et al. (2004) find that in 16 elliptical galaxies observed with the *Infrared Space Observatory* the dust masses are on average 10 times larger than those previously estimated from *Infrared Astronomy Satellite* observations. Most recently, Kaneda et al. (2005) have even detected polycyclic aromatic hydrocarbon emission features in four elliptical galaxies with the *Spitzer* Infrared Spectrograph. All these results suggest that the presence of a significant amount of interstellar material in elliptical galaxies is quite common, although its origin is still uncertain.

We attempt to determine the factor(s) that control the onset of nuclear activity by comparing the stellar population, central light distribution, and dust content for ellipticals with different levels of nuclear activity drawn from the Palomar spectroscopic survey of nearby galaxies (Ho et al. 1995, 1997a). This paper is organized as follows. The sample and analysis method are described in Sect. 2; the results of the stellar population synthesis

are presented in Sect. 3; the discussion and conclusions are given in Sect. 4.

2. Sample and method of analysis

The sample for this study was selected from the Palomar optical spectroscopic survey (Ho et al. 1995, 1997a), which comprises all nearby galaxies brighter than $B_T = 12.5$ mag in the northern hemisphere. It presents a fair representation of the local galaxy population. This is an ideal sample because it is statistically complete and contains both active ellipticals and inactive objects, drawn self-consistently from the same parent sample, that can serve as a control sample. The optical spectra are described in detail in Ho et al. (1995). Two spectra are available for each galaxy: the blue section covers ~4230–5110 Å with a *FWHM* spectral resolution of 4 Å, and the red section covers ~6210–6860 Å with a *FWHM* resolution of 2.5 Å. We select all ellipticals from the parent sample classified as either LINERs or absorption-line (inactive) sources, according to the criteria given in Ho et al. (1997a). We reject NGC 6702 because it only has the red spectrum, and two spheroidals (NGC 147 and NGC 205) because they have a different formation history than normal ellipticals (Kormendy 1985). We include NGC 221 (M 32), even though its absolute B-band magnitude is less than −18 mag, because it shares properties similar to those of normal ellipticals (Kormendy 1985; Ferguson & Binggeli 1994). Since the vast majority of the active sources are LINERs, we further removed 4 Seyferts and 5 transition objects. The final sample, whose global properties are summarized in Table 1, comprises 20 LINERs and 25 inactive ellipticals.

We modeled the stellar population of our sample using a modified version of the spectral population synthesis code, *starlight*[1], (Cid Fernandes et al. 2004; Gu et al. 2006). The code does a search for the best-fitting linear combination of 45 simple stellar populations (SSPs) – 15 ages and 3 metallicities ($0.2\,Z_\odot$, $1\,Z_\odot$, $2.5\,Z_\odot$) – provided by Bruzual & Charlot (2003) to match a given observed spectrum O_λ. The model SSP spectra cover 3200 Å to 9500 Å with a *FWHM* spectral resolution of ~3 Å (Bruzual & Charlot 2003, BC03 hereafter). The synthesized spectrum is given by (Cid Fernandes et al. 2004):

$$M_\lambda = M_{\lambda_0}\left(\sum_{i=1}^{N_*} x_i b_{i,\lambda} r_\lambda\right) \otimes G(v_*, \sigma_*), \quad (1)$$

where M_λ is the synthesized spectrum, M_{λ_0} is the synthesized flux at normalization wavelength λ_0 (4750 Å in this work), x_i is the contribution of the ith SSP, $b_{i,\lambda}$ is the spectrum of the ith SSP normalized at λ_0, and $r_\lambda = 10^{-0.4(A_\lambda - A_{\lambda_0})}$ is the reddening term. The Cardelli et al. (1989) extinction law with $R_V = 3.1$ is adopted. $G(v_*, \sigma_*)$ is the line-of-sight stellar velocity distribution, modeled as a Gaussian distribution centered at v_* and broadened by dispersion σ_*. The match between the model and the observed spectrum is calculated by $\chi^2(x, M_{\lambda_0}, A_V, v_*, \sigma_*) = \sum_{i=1}^{N_*}[(O_\lambda - M_\lambda)w_\lambda]^2$, where the weight spectrum, w_λ, is defined as the inverse of the noise of O_λ. For more details, see Cid Fernandes et al. (2004, 2005).

In order to account for the possibility of a weak AGN continuum (see Sect. 5.1 of Ho 2008), we add an additional power-law (PL) component ($f_\nu \propto \nu^{-1.5}$) during the fitting. Our fitting results show that, with the exception of NGC 315 and NGC 3193, the contribution from this PL component is negligible (less than 2%). Strong emission lines, such as Hβ, [O III] $\lambda\lambda$4959, 5007, Hα, and [N II] $\lambda\lambda$6548, 6583, are masked during the fitting process. The fitting procedure automatically determines a best-fitting stellar velocity dispersion (σ_*), taking into account the instrumental resolutions of both the Palomar and model library spectra. Cid Fernandes et al. (2004) estimate that the σ_* values derived from the code has a typical uncertainty of ~20 km s^{-1}.

Figures 1 and 2 show two fitting examples, for the LINER NGC 2768 and the inactive elliptical NGC 4648, respectively. The emission-line fluxes and line-intensity ratios measured in the residual spectra for the entire sample show excellent agreement (differences <10%) with those given in the original Palomar survey.

3. Results

3.1. Distance, luminosity, and stellar velocity dispersion

The distance and absolute blue magnitude of each galaxy, taken from Ho et al. (1997a), are listed in Table 1. In Fig. 3a we show the cumulative distribution of distance for the two subsamples. We find that LINERs and inactive ellipticals have similar distance distributions, with average distances of 29.9 and 25.7 Mpc, respectively. The LINER subsample contains the most distant object in the study, NGC 2832 at $D = 91.6$ Mpc; if we exclude this object, the average distance for the LINERs becomes 27.6 Mpc. We use the two-sample Kolmogorov-Smirnov (KS) statistical task *kolmov* in IRAF[2] to check whether the two subsamples are drawn from the same parent distribution. The probability of rejecting the null hypothesis that the two distributions are the same is $P_{\rm null} = 94\%$. Thus, distance effects between the two subsamples will not introduce any significant biases into our results.

The two subsamples also have very similar total luminosities, both in the optical and near-infrared bands. Figure 3b shows the cumulative distributions of absolute blue magnitude. LINERs have M_B ranging from −18.96 to −22.24 mag, with an average value of −20.69 mag, while inactive Es range from $M_B = -15.51$ to −21.64 mag, with an average value of −20.11 mag. A KS test yields $P_{\rm null} = 38\%$. We also derive absolute magnitudes in the K_s band, M_{K_s}, using data taken from the Two Micron All Sky Survey (Skrutskie et al. 2006). Figure 3c shows that the absolute K_s-band magnitudes of LINERs are similar to those of inactive Es: LINERs have an average $M_{K_s} = -24.54$ mag, to be compared with $M_{K_s} = -23.90$ mag for inactive Es. The near-infrared luminosity of the active sources have a slight tendency to be larger than those of the inactive sources, but a KS test yields $P_{\rm null} \approx 5\%$, which is formally only barely statistically significant. Moreover, this conclusion is not very robust. If we exclude the two most luminous objects from the active sample (NGC 315 and NGC 2832) and the least luminous object from the inactive sample (NGC 221), the significance drops to $P_{\rm null} \approx 14\%$.

Not surprisingly, the similarity between the two subsamples extends to the stellar velocity dispersions derived from our synthesis fitting (data in Col. 6 of Table 1), whose cumulative distributions are shown in Fig. 3d. For LINERs, the velocity dispersion ranges from 144 to 331 km s^{-1}, with an average value of $\langle\sigma_*\rangle = 251$ km s^{-1}; the corresponding values for inactive Es are $90 < \sigma_* < 349$ km s^{-1}, with $\langle\sigma_*\rangle = 211$ km s^{-1}. A KS test for

[1] http://www.starlight.ufsc.br/

[2] IRAF is distributed by the National Optical Astronomy Observatories, which are operated by the Association of Universities for Research in Astronomy, Inc., under cooperative agreement with the National Science Foundation.

Table 1. Global and central properties.

LINERs	D (Mpc)	M_B (mag)	M_{K_s} (mag)	Class	σ_* (km s^{-1})	A_V (mag)	Profile	Ref.	Dust Properties	Ref.
NGC 315	65.8	−22.22	−26.14	L1.9	322	0.42			Dust disk	2
NGC 1052	17.8	−19.90	−23.80	L1.9	240	0.04	core	1, 9	Has dust	3
NGC 2768	23.7	−21.17	−24.88	L2	170	0.32			Spiral dust lanes	4
NGC 2832	91.6	−22.24	−26.11	L2::	329	0.02	core	1, 10	No dust	5
NGC 3193	23.2	−20.10	−23.85	L2:	193	−0.02	core	1, 8	No dust	6
NGC 3226	23.4	−19.40	−23.28	L1.9	227	0.61			Dust disk	2
NGC 3379	8.1	−19.36	−23.27	L2/T2::	237	−0.17	core	1, 4	Dust ring or disk	4
NGC 3608	23.4	−20.16	−23.75	L2/S2:	218	−0.10	core	1, 4	Dust ring or disk	4
NGC 4261	35.1	−21.37	−25.46	L2	331	0.16	core	1, 3	Dust disk	2
NGC 4278	9.7	−18.96	−22.75	L1.9	269	−0.11	core	1, 4	Spiral dust lanes	4
NGC 4374	16.8	−21.12	−24.90	L2	246	0.96	core	1, 3	Dust lanes	3
NGC 4486	16.8	−21.64	−25.31	L2	328	0.04	core	1, 11	No dust	7
NGC 4494	9.7	−19.38	−22.94	L2::	144	0.14	PL	1, 8	Dust ring or disk	4
NGC 4589	30.0	−20.71	−24.63	L2	243	0.34	core	1, 4	Chaotic dust patches	4
NGC 4636	17.0	−20.72	−24.73	L1.9	215	0.14	core	1, 3	Dust lanes	7
NGC 5077	40.6	−20.83	−24.83	L1.9	266	0.04	core	1, 8	Dust filaments	6,8
NGC 5322	31.6	−21.46	−25.34	L2::	232	−0.08			Dust ring or disk	4
NGC 5813	28.5	−20.85	−24.86	L2:	257	0.21	core	1, 4	Dust disk	6
NGC 5982	38.7	−20.89	−24.79	L2::	267	−0.12	core	1, 4	No dust	2,3,6
NGC 7626	45.6	−21.23	−25.26	L2::	286	0.22	int	1, 3	Dust ring or disk	2,4
average	29.9	−20.69	−24.54		251	0.15				
rms	20.1	0.92	0.99		50	0.28				
Inactive Es	D (Mpc)	M_B (mag)	M_{K_s} (mag)	Class	σ_* (km s^{-1})	A_V (mag)	Profile	Ref.	Dust properties	Ref.
NGC 221	0.7	−15.51	−19.13	A	90	0.48	PL	3, 12	No dust	3, 12
NGC 821	23.2	−20.11	−23.93	A	205	0.31	int	1, 4	No dust	3, 4
NGC 2634	30.2	−19.69	−23.14	A	193	0.18	PL	1, 8	No dust	6
NGC 3348	37.8	−21.05	−24.92	A	221	0.32	core	1, 8	No dust	6
NGC 3377	8.1	−18.47	−22.10	A	166	0.36	PL	1, 4	Dust filaments	4, 6
NGC 3610	29.2	−20.79	−24.42	A	172	0.06	PL	1, 4	No dust	4
NGC 3613	32.9	−20.93	−24.58	A	219	0.19	core	1, 8	No dust	4
NGC 3640	24.2	−20.73	−24.40	A	196	0.27	core	1, 4	No dust	4, 6
NGC 4291	29.4	−20.09	−23.92	A	300	0.04	core	1, 4	No dust	3, 4, 6
NGC 4339	25.5	−19.72	−23.50	A	138	−0.01				
NGC 4365	16.8	−20.64	−24.49	A	251	0.30	core	1, 4	No dust	4, 6
NGC 4406	16.8	−21.39	−25.02	A	233	0.22	core	1, 4	No dust	4
NGC 4473	16.8	−20.10	−23.97	A	176	0.18	core	1, 4	No dust	4
NGC 4478	16.8	−18.92	−22.77	A	142	0.21	core	1, 4	No dust	4, 6
NGC 4564	16.8	−19.17	−23.19	A	160	0.24	PL	1, 8	No dust	6, 8
NGC 4621	16.8	−20.60	−24.38	A	245	0.14	PL	1, 4	No dust	4, 6
NGC 4648	27.5	−19.49	−23.35	A	222	0.26	PL	1, 8	Dust disk	6, 8
NGC 4649	16.8	−21.43	−25.39	A	349	0.23	core	1, 4	No dust	4
NGC 4660	16.8	−19.06	−22.92	A	198	0.27	PL	1, 4	No dust	4
NGC 4914	62.4	−21.64	−25.33	A	244	−0.04				
NGC 5557	42.6	−21.17	−25.07	A	290	−0.20	core	1, 4	No dust	4, 6
NGC 5576	26.4	−20.34	−24.28	A	211	0.08	core	1, 4	No dust	4, 6
NGC 5638	28.4	−20.21	−24.01	A	152	−0.32				
NGC 5831	28.5	−19.96	−23.84	A	167	0.13	PL	1, 8	No dust	6, 8
NGC 7619	50.7	−21.60	−25.49	A	337	0.24	core	1, 4	No dust	4
average	25.7	−20.11	−23.90		211	0.17				
rms	13.1	1.29	1.32		62	0.17				

Column (5): nuclear spectral classification from the Palomar survey Ho et al. (1997a): L = LINER, S = Seyfert, T = transition object, and A = absorption-line nucleus (inactive). The last two rows show the average value and rms of each column.
References: 1. Lauer et al. (2007); 2. González Delgado et al. (2008); 3. Ravindranath et al. (2001); 4. Lauer et al. (2005); 5. Martel et al. (2004); 6. Tran et al. (2001); 7. van Dokkum & Franx (1995); 8. Rest et al. (2001); 9. Quillen et al. (2000); 10. Laine et al. (2003); 11. Lauer et al. (1995); 12. Faber et al. (1997).

the full sample yields $P_{\rm null} \approx 3\%$, but the significance drops to $P_{\rm null} \approx 9\%$ after excluding NGC 315 and NGC 2832 from the LINER sample and NGC 221 from the inactive sample.

3.2. Stellar populations

As mentioned in Sect. 2, our spectral library covers 15 ages and 3 metallicities, which produce a total of 45 SSPs. Here we rebin the 45 SSPs into 5 components according to age: I ($10^6 \le t < 10^7$ yr); II ($10^7 \le t < 10^8$ yr); III ($10^8 \le t < 10^9$ yr); IV ($10^9 \le t < 10^{10}$ yr); and V ($t \ge 10^{10}$ yr). We derive the light-weighted mean stellar age using the formula in Cid Fernandes et al. (2005):

$$\langle \log t_* \rangle_{\rm L} = \sum_{i=1}^{45} x_i \log t_i, \qquad (2)$$

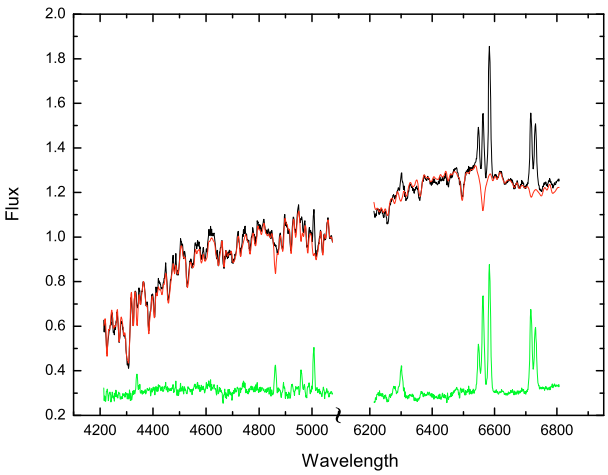

Fig. 1. Synthesis results for the LINER NGC 2768. The flux is normalized at 4750 Å. The black line is the observed spectrum; the red line is the synthesized spectrum; and the green line is the residual spectrum after subtracting the synthesized spectrum from the observed spectrum. The vertical scale has been shifted arbitrarily. There are no data in the region ~5110–6210 Å.

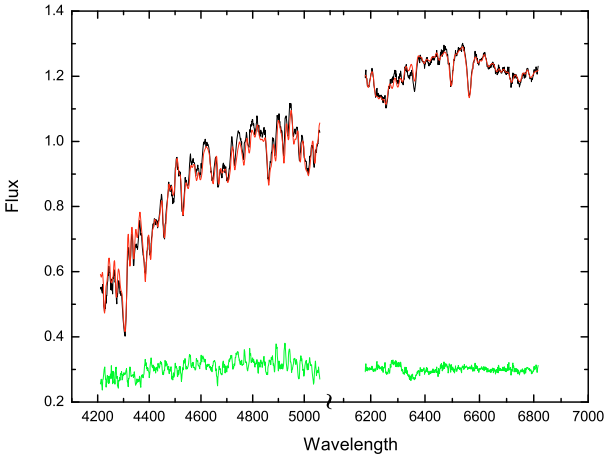

Fig. 2. Same as Fig. 1, but for the inactive elliptical NGC 4648.

where x_i denotes the contribution of the ith SSP and t_i its corresponding age. Similarly, the light-weighted mean stellar metallicity is computed from

$$\langle Z_* \rangle_L = \sum_{i=1}^{45} x_i Z_i, \quad (3)$$

where x_i represents the contribution of the ith SSP with metallicity Z_i. The synthesis results are presented in Table 2. Columns (2) through (6) give the fractional light contribution from the AGN PL component and from stellar populations I–V. Columns (7) and (8) list the mean stellar age and metallicity.

Figure 4 shows the contribution of each stellar population for the LINER (upper panel) and inactive E (lower panel) subsamples. It is clear that young and intermediate-age stellar populations contribute very little to the total flux for either group. For LINERs, stellar population I, II, and III contribute only <1%, 2%, and <1%, respectively; for inactive Es, the corresponding values are 1%, 2%, and <1%. Most of the optical light is dominated by an old population. The mean contribution from stellar population IV and V are 11% and 86% for LINERs, and 20% and 76% for inactive Es.

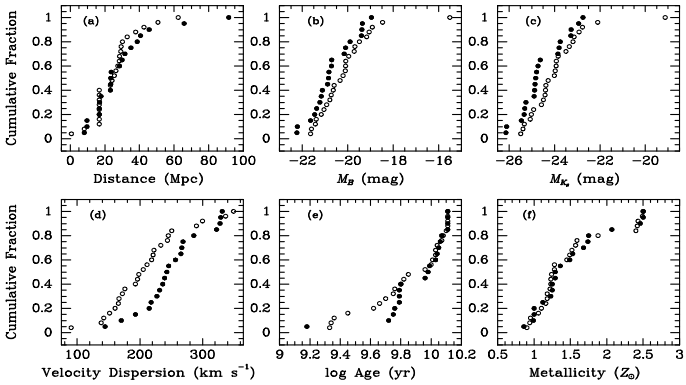

Fig. 3. Cumulative distribution of **a)** distance, **b)** absolute blue magnitude, **c)** absolute K_s-band magnitude, **d)** central stellar velocity dispersion, **e)** mean stellar age, and **f)** mean stellar metallicity. Active (LINER) and inactive ellipticals are labeled as filled and open circles, respectively.

Figure 3e shows the cumulative distribution of mean stellar age for LINERs and inactive Es. Their average age is 8.1 Gyr and 7.1 Gyr, respectively. The only exception is the LINER NGC 4374, which has a dominant 1.4 Gyr old stellar population that contributes 89% of the light. Our stellar population synthesis suggests that LINERs and inactive Es have very similar stellar populations, both lacking young and intermediate-age populations. A KS test yields $P_{\rm null}$ = 31%(68%, NGC 221 excluded). The similarity of the stellar populations of the two groups further extends to the derived metallicities (Fig. 3f): the average metallicity for both subsamples is ~1.5 $Z_\odot$.

3.3. Central light profile

Central surface brightness profiles carry many clues on the formation and evolutionary history of the galaxy (Faber et al. 1997; Lauer et al. 2005). We compare the surface brightness profiles of LINERs and inactive Es derived from *Hubble Space Telescope (HST)* images, and try to find whether there is any difference between the two subsamples. The high angular resolution of *HST* is crucial to derive robust central profiles of galaxies.

Lauer et al. (1995) classified the central surface brightness profiles of early-type galaxies into two types. Core galaxies have central light distributions that turnover from a steep outer profile to a shallower cusp interior to some break radius. Power-law galaxies, on the other hand, display continuously rising inner profiles down to the resolution of *HST*. The two classes correlate with the large-scale properties of the galaxies. Core galaxies are invariably luminous giant ellipticals that are slowly rotating and show boxy isophotes; power-law galaxies occupy more intermediate luminosities, rapidly rotate, and show disky isophotes. The physical implications of these two classes for their formation histories are discussed in detail in Faber et al. (1997).

Published *HST* surface brightness profiles and classifications are available for most of our sample, as documented in Table 1. Among the 16 LINERs with profile classifications, 14 (88%) are core galaxies; only one galaxy, NGC 4494, is classified as a power-law system, and another, NGC 7626, has an intermediate profile. Four (NGC 315, 2768, 3226, and 5322) are too dusty to determine their profiles reliably and cannot be classified. However, for the inactive galaxies, only 12 out of 22 (55%) have cores, whereas 9 (41%) have power-law profiles; NGC 821 has an intermediate classification, and three others lack data.

Table 2. Synthesis results.

LINERs	PL (%)	I (%)	II (%)	III (%)	IV (%)	V (%)	log age (yr)	Metallicity ($Z_\odot$)
NGC 315	7	2	<1	<1	<1	92	9.79	1.29
NGC 1052	<1	<1	<1	<1	11	89	10.03	1.53
NGC 2768	<1	<1	<1	<1	37	63	9.79	2.07
NGC 2832	<1	<1	<1	<1	<1	99	10.11	1.29
NGC 3193	9	<1	<1	<1	<1	91	9.72	1.12
NGC 3226	<1	<1	<1	<1	72	28	9.79	1.00
NGC 3379	<1	<1	<1	<1	<1	99	10.11	1.68
NGC 3608	2	<1	<1	<1	<1	98	10.05	1.23
NGC 4261	<1	<1	<1	<1	5	95	10.06	1.49
NGC 4278	<1	1	<1	<1	<1	99	10.07	1.75
NGC 4374	<1	<1	2	<1	90	8	9.18	2.46
NGC 4486	<1	2	1	<1	<1	96	9.99	0.86
NGC 4494	<1	<1	7	<1	11	83	9.80	1.25
NGC 4589	<1	<1	11	<1	1	88	9.76	2.50
NGC 4636	<1	<1	<1	<1	<1	99	10.04	1.00
NGC 5077	<1	4	<1	<1	<1	96	9.96	1.74
NGC 5322	<1	<1	12	<1	<1	88	9.75	2.50
NGC 5813	<1	<1	<1	<1	<1	99	10.11	1.36
NGC 5982	1	<1	<1	<1	<1	98	9.98	0.99
NGC 7626	<1	<1	<1	<1	<1	99	10.11	1.25
average	1.0	0.4	1.7	<1	11	86	9.91	1.52
rms	2.5	1.0	3.6	<1	25	24	0.22	0.51
Inactive Es		I (%)	II (%)	III (%)	IV (%)	V (%)	log age (yr)	Metallicity ($Z_\odot$)
NGC 221		1	<1	4	94	<1	9.33	1.88
NGC 821		<1	<1	<1	<1	99	10.10	1.18
NGC 2634		1	<1	<1	1	98	10.07	1.28
NGC 3348		<1	4	<1	<1	96	10.01	2.50
NGC 3377		<1	8	<1	11	82	9.34	2.49
NGC 3610		<1	7	<1	56	37	9.36	2.40
NGC 3613		<1	3	<1	24	73	9.80	1.57
NGC 3640		<1	<1	<1	30	70	9.82	1.45
NGC 4291		4	2	<1	29	65	9.70	2.42
NGC 4339		<1	3	<1	1	95	9.96	1.59
NGC 4365		<1	12	<1	<1	88	9.75	1.28
NGC 4406		2	<1	<1	<1	98	10.04	0.94
NGC 4473		<1	<1	<1	29	71	9.85	1.49
NGC 4478		<1	<1	<1	99	<1	9.66	0.90
NGC 4564		3	<1	<1	<1	97	10.00	1.10
NGC 4621		2	<1	<1	<1	98	10.03	1.18
NGC 4648		<1	<1	<1	<1	99	10.11	1.23
NGC 4649		<1	<1	<1	3	96	10.03	0.95
NGC 4660		<1	5	<1	15	80	9.76	1.23
NGC 4914		<1	8	<5	87	<1	9.45	2.43
NGC 5557		<1	<1	<1	1	99	10.08	1.06
NGC 5576		2	6	<1	25	66	9.62	1.52
NGC 5638		<1	<1	<1	<1	99	10.11	1.16
NGC 5831		<1	<1	<1	<1	99	10.11	1.22
NGC 7619		<1	<1	<1	<1	99	10.11	1.24
average		0.6	2.3	0.4	20	76	9.85	1.51
rms		1.1	3.4	1.3	31	32	0.26	0.53

Columns (2)–(7) list the fractional contribution to the total flux by the PL and by stellar populations I, II, III, IV, and V, respectively. Contributions less than 1% are listed as upper limits. Column (8) gives the mean stellar age, and Col. (9) gives the mean metallicity. The last two rows show the average value and rms of each column.

3.4. Central dust content

Elliptical galaxies are traditionally viewed as structurally simple systems composed of old stars and lacking in cold gas and dust. Recent observations, especially from *HST* images, show unambiguous evidence that many ellipticals exhibit central dust structures (van Dokkum & Franx 1995; Tran et al. 2001; Lauer et al. 2005). Lauer et al. (2005) suggested a dust-settling sequence in early-type galaxies: the dust starts off poorly organized, then gradually settles down to the center and forms dusty rings or disks. The origin of gas and dust in elliptical galaxies is not well understood. Two possibilities are frequently discussed – an internal origin from stellar mass loss or an external origin from accretion of a gas-rich companion (Lauer et al. 2005; Sarzi et al. 2006). Although we do not have detailed kinematic information on our galaxies, they are morphologically regular and do not show obvious signs of recent interactions or mergers.

We compare the dust properties of LINERs and inactive Es in our sample. Information on the central dust properties, gathered from a literature search, is summarized in Table 1. Among

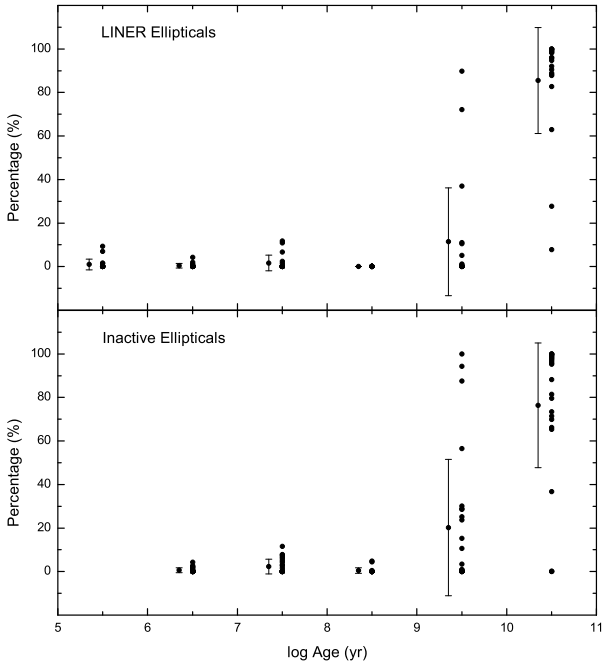

Fig. 4. The fractional contribution to the total flux of each stellar population for LINERs (*upper panel*) and inactive ellipticals (*lower panel*). The abscissa gives the logarithm of the age, where 5.5 corresponds to the AGN PL component; 6.5, 7.5, 8.5, 9.5, and 10.5 correspond to stellar populations I, II, III, IV, and V, respectively. The point and error bar to the left of each population indicate the average fraction and rms, respectively. We did not fit a PL component to the inactive ellipticals.

the LINERs, 16 out of 20 (80%) have detected central dust structures. In stark contrast, only 2 out of 22 (9%) inactive ellipticals with suitable *HST* data show dust features. Interestingly, the optical extinction derived from the population synthesis analysis (A_V in Table 1) shows no clear correspondence with the presence or absence of dust features inferred from the *HST* images; $\langle A_V(\mathrm{LINERs})\rangle - \langle A_V(\mathrm{inactive})\rangle = -0.02 \pm 0.33$. This suggests that the dust features seen in the *HST* images lie on significantly smaller scales than the bulk of the stars sampled by the spectra.

4. Discussion and conclusions

Analyzing a statistically complete sample of 45 elliptical galaxies from the Palomar spectroscopic survey of nearby galaxies, comprising 20 LINERs and 25 inactive members, we show that galaxies hosting LINER nuclei, compared to systems lacking optical evidence for nuclear activity, have very similar stellar properties, both on global and nuclear scales. Specifically, we find that the two galaxy subgroups have essentially indistinguishable total optical and near-infrared luminosities, central stellar velocity dispersions, and luminosity-weighted mean stellar ages and metallicities on nuclear ($\lesssim$300 pc) scales. The lack of young or intermediate-age stars in LINERs strongly rule out starburst and post-starburst models for the excitation of LINER-like emission, further strengthening the proposition that LINERs are low-luminosity AGNs (Ho 2008).

Our results are qualitatively consistent with those from previous studies of the Palomar survey. Ho et al. (2003) systematically investigated the stellar population of the emission-line nuclei in the Palomar survey and found that LINERs generally contain evolved stellar populations. Other evidence concerning the old ages of the nuclear stellar population in nearby low-luminosity AGNs is summarized in Ho (2008). Ho et al., however, did not derive detailed ages or metallicities from a population synthesis analysis. This work is the first quantitative analysis of its kind for the Palomar survey. On the other hand, studies of larger samples of LINERs drawn from the Sloan Digital Sky Survey (SDSS) reach somewhat different conclusions. While LINERs on average have older stars than Seyferts (Kewley et al. 2006), Graves et al. (2007) and Schawinski et al. (2007) show that LINERs have a tendency to exhibit somewhat younger populations (by ~3 Gyr) compared to inactive early-type galaxies devoid of emission lines. The differences between our results and those derived from SDSS can plausibly be attributed to a combination of several effects. First, the SDSS sources have redshifts $z \approx 0.05$–0.1, much more distant than the Palomar galaxies. As discussed by Ho (2008), aperture effects render the interpretation of LINER emission in distant galaxies somewhat problematic. Second, the stellar population analysis method of this paper differs from that used in the SDSS studies, and it is unclear if there are residual systematic discrepancies between the different methods. Third, our grid of SSP spectra may be too coarse to be able to resolve the small age difference reported in the SDSS studies. Finally, we note that the spectral range of the Palomar data is more limited than that of SDSS.

Surprisingly, we find that LINER host galaxies have a greater tendency to exhibit central core light profiles. Lauer et al. (2005) suggest that core galaxies are more luminous, more massive, and may be older than power-law galaxies, seemingly at odds with our results. Considering the modest size of our sample, however, and the large scatter in the statistical correlations between profile type and global properties, this disagreement is not too alarming.

By far the clearest distinction between active and inactive ellipticals is that the former has a much higher likelihood of containing circumnuclear dust. This finding is in excellent agreement with that of Lauer et al. (2005), who also found a strong correlation between the incidence of nebular line emission – which in ellipticals invariably signifies a LINER classification (Ho 2008) – and central dust features: 90% of emission-line nuclei show detected central dust structures, to be compared with just 4% for the lineless systems. Ravindranath et al. (2001) similarly suggested a connection between Hα emission and dust features, and the tendency for LINERs to be more dusty. Recently, Simões Lopes et al. (2007) presented strong evidence that circumnuclear dust is correlated with AGN activity in early-type galaxies. Among 34 early-type galaxies classified as AGNs, all show circumnuclear dust structures, to be compared with only 26% in the control sample of inactive systems.

Taken collectively, the above evidence suggests that ellipticals with weakly active, LINER nuclei are more gas-rich than their inactive counterparts. Given the lower stellar density in the cores, we actually expect *less* cold gas accumulation from stellar mass loss, not more, among the LINER hosts (see, e.g., Soria et al. 2006). On the other hand, massive ellipticals are surrounded by hot X-ray halos (e.g., Jones et al. 2002), whose cooling time is sufficiently short that cooling flows should develop. We speculate that the central dust features in core-type LINER ellipticals may partly originate from cooling condensations in the X-ray-emitting gas. The "extra" cold gas and dust, in combination with direct spherical accretion from the hot gas itself, may be responsible for sustaining the weak nuclear activity. Perhaps elliptical galaxies with LINER nuclei identify the subclass of early-type galaxies in which this mode of accretion is significant.

Acknowledgements. We thank an anonymous referee for comments that led to significant improvements in the paper. The *starlight* project is supported

by the Brazilian agencies CNPq, CAPES and FAPESP and by the France-Brazil CAPES/Cofecub program. This work is supported by Program for New Century Excellent Talents in University (NCET), the National Natural Science Foundation of China under grants 10221001 and 10633040, the National Basic Research Program (973 program No. 2007CB815405), and the Carnegie Institution of Washington. This research has made use of NASA's Astrophysics Data System Bibliographic Services and the NASA/IPAC Extragalactic Database (NED), which is operated by the Jet Propulsion Laboratory, California Institute of Technology, under contract with the National Aeronautics and Space Administration. This publication makes use of data products from the Two Micron All Sky Survey, which is a joint project of the University of Massachusetts and the Infrared Processing and Analysis Center/California Institute of Technology, funded by the National Aeronautics and Space Administration and the National Science Foundation.

References

Barth, A. J., Filippenko, A. V., & Moran, E. C. 1999a, ApJ, 515, L61
Barth, A. J., Filippenko, A. V., & Moran, E. C. 1999b, ApJ, 525, 673
Barth, A. J., Ho, L. C., Filippenko, A. V., Rix, H.-W., & Sargent, W. L. W. 2001, ApJ, 546, 205
Bruzual, G., & Charlot, S. 2003, MNRAS, 344, 1000
Cardelli, J. A., Clayton, G. C., & Mathis, J. S. 1989, ApJ, 345, 245
Cid Fernandes, R., Gu, Q., Melnick, J., et al. 2004, MNRAS, 355, 273
Cid Fernandes, R., Mateus, A., Sodré, L., Stasińska, G., & Gomes, J. M. 2005, MNRAS, 358, 363
Faber, S. M., Tremaine, S., Ajhar, E. A., et al. 1997, AJ, 114, 1771
Ferguson, H. C., & Binggeli, B. 1994, A&AR, 6, 67
Ferrarese, L., & Merritt, D. 2000, ApJ, 539, L9
Gebhardt, K., Bender, R., Bower, G., et al. 2000, ApJ, 539, L13
González Delgado, R. M., Pérez, E., Cid Fernandes, R., & Schmitt, H. 2008, AJ, 135, 747
Graves, G. J., Faber, S. M., Schiavon, R. P., & Yan, R. 2007, ApJ, 671, 243
Gu, Q., Melnick, J., Cid Fernandes, R., et al. 2006, MNRAS, 366, 480
Heckman, T. M. 1980, A&A, 87, 152
Ho, L. C. 2008, ARA&A, in press [arXiv:0803.2268]
Ho, L. C., Filippenko, A. V., & Sargent, W. L. W. 1995, ApJS, 98, 477
Ho, L. C., Filippenko, A. V., & Sargent, W. L. W. 1997a, ApJS, 112, 315
Ho, L. C., Filippenko, A. V., Sargent, W. L. W., & Peng, C. Y. 1997b, ApJS, 112, 391
Ho, L. C., Rudnick, G., Rix, H.-W., et al. 2000, ApJ, 541, 120
Ho, L. C., Feigelson, E. D., Townsley, L. K., et al. 2001, ApJ, 549, L51
Ho, L. C., Filippenko, A. V., & Sargent, W. L. W. 2003, ApJ, 583, 159
Jones, C., Forman, W., Vikhlinin, A., et al. 2002, ApJ, 567, L115
Kaneda, H., Onaka, T., & Sakon, I. 2005, ApJ, 632, L83
Kewley, L. J., Groves, B., Kauffmann, G., & Heckman, T. 2006, MNRAS, 372, 961
Knapp, G. R., Guhathakurta, P., Kim, D.-W., & Jura, M. A. 1989, ApJS, 70, 329
Kormendy, J. 1985, ApJ, 295, 73
Laine, S., van der Marel, R. P., Lauer, T. R., et al. 2003, AJ, 125, 478
Lauer, T. R., Ajhar, E. A., Byun, Y.-I., et al. 1995, AJ, 110, 2622
Lauer, T. R., Faber, S. M., Gebhardt, K., et al. 2005, AJ, 129, 2138
Lauer, T. R., Gebhardt, K., Faber, S. M., et al. 2007, ApJ, 664, 226
Maoz, D., Nagar, N. M., Falcke, H., & Wilson, A. S. 2005, ApJ, 625, 699
Martel, A. R., Ford, H. C., Bradley, L. D., et al. 2004, AJ, 128, 2758
Nagar, N. M., Falcke, H., & Wilson, A. S. 2005, A&A, 435, 521
Phillips, M. M., Jenkins, C. R., Dopita, M. A., Sadler, E. M., & Binette, L. 1986, AJ, 91, 1062
Quillen, A. C., Bower, G. A., & Stritzinger, M. 2000, ApJS, 128, 85
Ravindranath, S., Ho, L. C., Peng, C. Y., Filippenko, A. V., & Sargent, W. L. W. 2001, AJ, 122, 653
Rest, A., van den Bosch, F. C., Jaffe, W., et al. 2001, AJ, 121, 2431
Sarzi, M., Falcón-Barroso, J., Davies, R. L., et al. 2006, MNRAS, 366, 1151
Schawinski, K., Thomas, D., Sarzi, M., et al. 2007, MNRAS, 382, 1415
Soria, R., Graham, A. W., Fabbiano, G., et al. 2006, ApJ, 640, 143
Shields, J. C. 1991, AJ, 102, 1314
Shields, J. C., Rix, H.-W., McIntosh, D. H., et al. 2000, ApJ, 534, L27
Simões Lopes, R. D., Storchi-Bergmann, T., de Fátima de, O., Saraiva, M., & Martini, P. 2007, ApJ, 655, 718
Skrutskie, M. F., Cutri, R. M., Stiening, R., et al. 2006, AJ, 131, 1163
Temi, P., Brighenti, F., Mathews, W. G., & Bregman, J. D. 2004, ApJS, 151, 237
Terashima, Y., & Wilson, A. S. 2003, ApJ, 583, 145
Tran, H. D., Tsvetanov, Z., Ford, H. C., et al. 2001, AJ, 121, 2928
van Dokkum, P. G., & Franx, M. 1995, AJ, 110, 2027